Chalcogenide Letters Vol. 20, No. 12, December 2023, p. 903 - 913

Theoretical study on structural, electronic structure, elastic and optical properties of α-Cu_2S

Y. Jie[a], S. R. Zhang[a,*], H. J. Hou[b], L. H. Xie[c]
[a]*School of Physics, Electronics and Intelligent Manufacturing, Huaihua University, Huaihua, 418008, China*
[b]*School of Materials Engineering, Yancheng Institute of Technology, Yancheng, 224051, China*
[c]*School of Physics and Electronic Engineering, Sichuan Normal University, Chengdu, 610066, China*

Based on the first-principles method, the electronic structure, mechanical and optical properties of α-Cu_2S are studied. The results show that the optimized structural parameters are in good agreement with the experimental value. The energy band structure and density of states of α-Cu_2S is obtained by calculation and analysis. The mechanical properties such as bulk modulus, shear modulus, Young's modulus and Poisson's ratio are calculated at different pressures. At last, the dielectric function, refractive index, absorption coefficient and reflectivity of α-Cu_2S is analyzed. It was found that α-Cu_2S is a direct bandgap with a band gap of 1.2 eV and has good potential for optoelectronic applications.

(Received September 7, 2023; Accepted December 18, 2023)

Keywords: α-Cu_2S, Electronic structure, Elastic, Optical properties

1. Introduction

Copper-based compounds Cu_2Ch (Ch = O, S, Se, Te), $CuMCh_2$(M = Sb, Bi; Ch = S, Se, Te), $Cu_2ZnSnCh_4$(Ch= S, Se) are potential solar energy conversion materials[1-7]. Their are a new type of inorganic solar cell materials that have attracted much attention in recent years. The band gaps of these list of semiconductor materials are very well matched with the sunlight, and they are all direct band gaps, light absorption performance is good, the most important is that its components are non-toxic. Thus, the copper-based chemicals Cu_2Ch (CH = O, S, Se, Te), $CuMCh_2$(M = Sb, Bi; Ch = S, Se, Te), $Cu_2ZnSnCh4$ (Ch= S, Se) are ideal photovoltaics list of semiconductor materials. Among copper-based compounds, Cu_2S semiconductor is a good solar energy absorbing material because of its safety, low cost and ideal band gap of 1.2-2.5 eV. Because it is a P-type semiconductor and can absorb part of the visible light, it is considered as a very promising material in the field of solar energy conversion. At the same time, Cu_2S is of great importance in photovoltaic, thermoelectric and solar panel display devices. Below 103 °C, Cu_2S exists as monoclinal low chalcocite (γ-Cu_2S). In the temperature range of 103-435 °C, the most

* Corresponding author: zefer1979@163.com
https://doi.org/10.15251/CL.2023.2012.903

stable phase is hexagonal pyroxene (β-Cu_2S), which transforms into cubic (α-Cu_2S) above 435 °C. α-Cu_2S has a regular anti-calcium fluoride crystal structure, and the S atom occupies the 4a Wyckoff's (0, 0, 0) position, which ensures that the electronic carriers move unperturbed through the lattice nodes, the highly mobile copper ions forming the cationic sublattice can“Jump” between the equivalent positions in the lattice at short time intervals. However, there are many properties, such as electronic structure, elasticity, optical, etc., which are not well known in previous studies. For example, although we have done extensive research on the electronic properties of α-Cu_2S, the range of available data is also extensive. But for elastic properties, we only have limited information. Moreover, the two parameters of pressure and temperature play an important role in adjusting the physical properties of materials. Therefore, the main purpose of this study is to use density functional theory to calculate the structure, electronic properties, elastic and optical properties of α-Cu_2S.

2. Calculation methods

In this work, all the calculations are performed using the CASTEP code, based on the density functional theory(DFT) [8]. The Vanderbilt ultrasoft pseudopotential [9] is used with the cutoff energy of 450.0 eV for the considered structure. The k point meshes of 4×4×4 for cubic structure α-Cu_2S is generated using the Monkhorst-Pack scheme. The electronic exchange-correlation potentials are described within within the generalized gradient approximation (GGA) proposed by Perdew et al.[10].

3. Results and discussion

3.1. Structural optimization

The structure chosen in this work is cubic α-Cu_2S (Fig. 1), the space group is $Fm\bar{3}m$(No.225), and Cu atomic coordinates: (0.25, 0.25, 0.25), S atomic coordinates: (0, 0 , 0) .

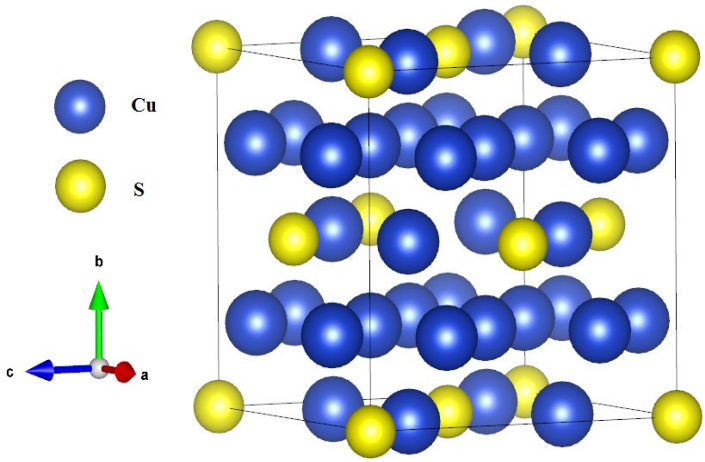

Fig. 1. Structural feature of α-Cu_2S.

Table 1. The present calculated lattice constants of α-Cu_2S determined by LDA, GGA-PBE, GGA-RPBE, GGA-PW91, GGA-PW91 and WC-GGA compared with experimental value.

	LDA	PBE-GGA	RPBE-GGA	PW91-GGA	WC-GGA	Experimental [11]
$a = b = c$ (Å)	5.410	5.579	5.654	5.585	5.484	5.570
Relative error	2.87%	0.16%	1.51%	0.27%	1.54%	

It can be concluded from the Table 1 that the minimum relative error of the calculated lattice constant *a* is 0.16% when the generalized gradient approximation (GGA) exchange correlation potential is PBE. The largest relative error was calculated using Local-density approximation (LDA), at 2.87%. Because the relative error between the results calculated by PBE-GGA method and the experimental values is the least, it is more close to the experimental value, which shows that the reliability of the results calculated by this method is higher, therefore, we use this method in the following research calculation process. Then, we use PBE-GGA method to optimize the cell when it is 0 GPa, 2GPa, 4 GPa, 6 GPa, 8 GPa, 10 GPa respectively. As can be seen from Fig. 2, the lattice constant *a* of α-Cu_2S decreases with increasing pressure, so the total cell volume decreases with increasing pressure. The reason for this result is that the interaction force between α-Cu_2S atoms increases under increasing external pressure, which causes the crystal to be compressed and the bond length to be shortened.

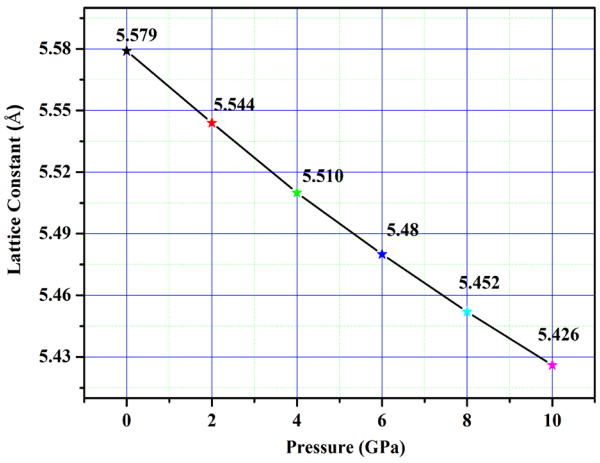

Fig. 2. Lattice constant a of α-Cu_2S at different pressures.

3.2. Electronic structure

The lattice constant of α-Cu_2S was optimized at zero pressure, and the band structure was obtained by GGA-PBE method (as shown in Fig. 3). It can be seen that the band gap is 0.029 eV, but it is quite different from 1.2 eV [12]. It is well known that the reason for this difference is that GGA-based Density functional theory (DFT), when calculating semiconductors or insulators, especially in systems with more severe electron interactions (such as α-Cu_2S), if the excited state

can not be described accurately, the band gap value will be seriously underestimated. However, the DFT-GGA method can well describe the electronic structure and many physical properties of materials. Therefore, the band structure described in Fig. 4 is in good agreement with the experimental results.

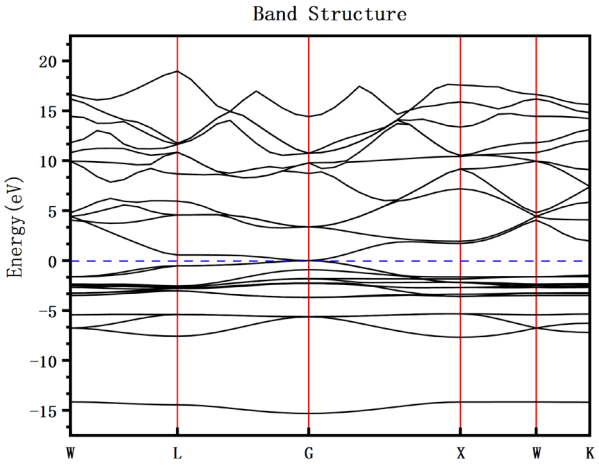

Fig. 3. The electronic band structure of of α-Cu_2S.

In this work, in order to adjust the band gap value, we introduce a scissors operator to modify the band gap (correction factor x = 1.171 eV), and the corrected band gap value is consistent with the experimental value of 1.2 eV.

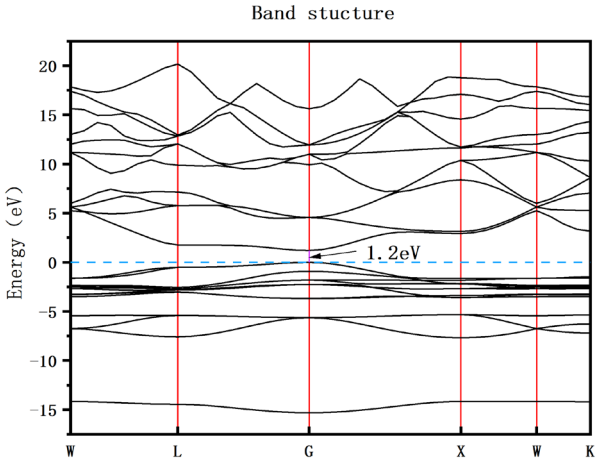

Fig. 4. Band structure of α-Cu_2S after modification by scissors operator.

As can be seen from Fig. 4, both the top and the bottom of the modified valence band are at the G-point, resulting in a direct bandgap band gap of 1.2 eV for α-Cu_2S.

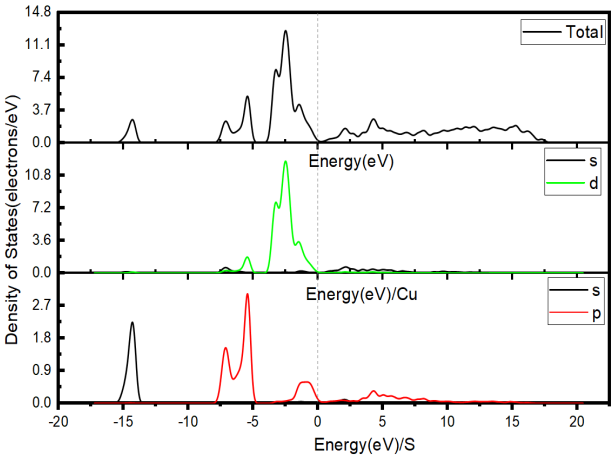

Fig. 5. The partial density of states and total density of states of α-Cu_2S.

The partial density of states of α-Cu_2S and total density of state are obtained, as shown in Fig. 5. The valence electron structure of Cu is $3d^{10}4S^1$ and that of S is $3S^23P^4$. The uppermost valence band width of α-Cu_2S is about -3.96 eV ~ -0.02 eV, and there are three peaks at -3.24 eV, -2.24 eV and -1.43 eV. The first two peaks are mainly derived from the d-orbitals of Cu atoms. The last peak mainly comes from the d orbitals of the Cu atoms and hybridizes the p orbitals of the S atoms, the valence band width of the middle part is about -7.88 eV ~ -4.92 eV, and there are two peaks at -7.13 eV and -5.39 eV, the former is derived from the p orbitals of S, while the latter is the p orbitals of the hybrid s of Cu d orbitals, the width of valence band at the bottom is about -15.41 eV~ -13.75 eV, and there is a peak at -14.28 eV, the contribution is made by the p orbitals of S.

3.3. Elastic properties

α-Cu_2S belongs to cubic system, so it has three independent components, which are C_{11}, C_{12}, C_{44} respectively. Using these elastic constants, we can determine the mechanical stability of the crystal. According to the Born stability criterion, the criterion for the elastic stability of a cubic system under pressure is [13]

$$(C_{11}+2C_{12}+P)>0;\ (C_{44}-P)>0;\ (C_{11}-C_{12}-2P)>0 \quad (1)$$

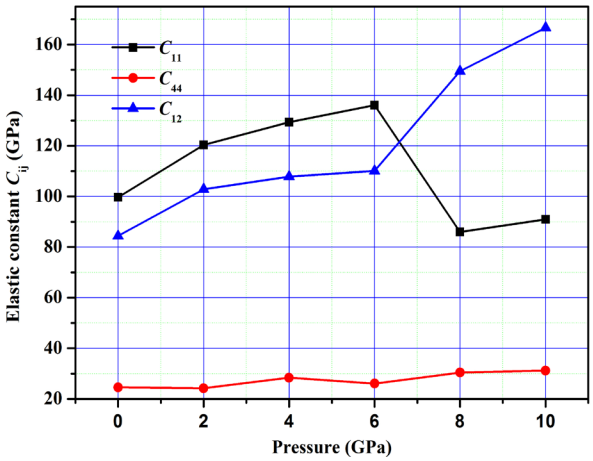

Fig. 6. Effect of pressure on the C_{ij} of α-Cu_2S as a function of pressure.

Fig. 6 shows that C_{11} increases in the range of 0-6 GPa, but decreases in the range of 6-10 GPa in the three elastic constants (C_{11}, C_{12}, C_{44}) with increasing pressure, and C_{12} increases with increasing pressure, but in the range of 6-10 GPa, the increase amplitude of C_{44} is steeply increased, and the change ratio of C_{44} with pressure is not obvious, the overall increase trend is still present, which shows that the sensitivity of C_{44} to pressure is far less than the other two independent elastic constants. From the data shown in Table 2, it can be seen that α-Cu_2S is mechanical stability at 0-6 GPa, and the elastic constant C_{ij} increases with the increase of pressure, the results show that the compressibility of the crystals decreases with the increase of pressure, but when the pressure is over 6 GPa, the calculated results no longer satisfy the elastic stability criterion, the results show that the crystal structure of α-Cu_2S is not stable when the pressure of α-Cu_2S is higher than 6 GPa, and there is possibility of phase transition. Because there is no comparison between the theoretical and experimental values, we can only infer from the calculated results that the limiting pressure of α-Cu_2S during phase transition is between 6 GPa and 8 GPa.

Table 2. Calculated elastic constants C_{ij} (GPa) and $S_{ij}(10^{-3}GPa^{-1})$ of α-Cu_2S at 0, 2, 4, 6, 8 and 10 GPa, respectively.

Pressure(GPa)	C_{11}	C_{44}	C_{12}	S_{11}	S_{44}	S_{12}
0	99.70	24.57	84.39	44.78	40.69	84.39
2	120.34	24.21	102.84	39.11	41.29	102.84
4	129.30	28.4	107.88	32.08	35.21	107.88
6	136.02	26.06	110.11	42.87	47.47	110.11
8	85.94	30.42	149.48	-9.62	32.85	149.48
10	90.95	31.22	166.65	-8.02	32.02	166.65

Then, when the α-Cu_2S crystal is in the elastic stable state range (0-6 GPa), according to the elastic constants at different pressures, Voigt-Reuss-Hill [14-16] method was used to calculate and analyze the bulk modulus B, shear modulus G, Young's modulus E and Poisson's ratio υ of the crystal, which are presented in Table 3. According to Voigt-Reuss-Hill approximation, the bulk modulus B, and shear modulus G are calculated as follows:

$$B_V = B_R = \frac{C_{11} + 2C_{12}}{3} \tag{2}$$

$$B_H = \frac{B_V + B_R}{2} \tag{3}$$

$$G_V = \frac{C_{11} - C_{12} + 3C_{44}}{5} \tag{4}$$

$$G_R = \frac{5(C_{11} - C_{12})C_{44}}{4C_{44} + 3(C_{11} - C_{12})} \tag{5}$$

$$G_H = \frac{G_V + G_R}{2} \tag{6}$$

Young's modulus E and Poisson ratio υ

$$E = \frac{9BG}{3B+G} \tag{7}$$

$$\upsilon = \frac{1}{2}\left(1-\frac{E}{3B}\right) \tag{8}$$

As shown in Table 3 and Fig. 7, *B*, *G*, and *E* increase monotonically with increasing pressure. Because the bulk modulus *B* is much larger than the shear modulus *G* at each pressure, the shear resistance of α-Cu_2S crystal is much weaker than that of compression. Young's modulus *E* is used to describe the deformation resistance of a solid material. From Fig. 7, Young's modulus *E* increases with increasing pressure. This means that the stiffness of the crystal increases with increasing pressure.

Table 3. B (GPa), G (GPa), E(GPa), Poisson ratio υ, B/G of α-Cu_2S at different pressures.

Pressure（GPa）	*B*	*G*	*E*	*υ*	*B*/*G*
0	89.49	15.42	43.76	0.418	5.802
2	108.68	16.11	46.05	0.429	6.746
4	115.02	19.21	54.60	0.431	5.986
6	118.75	19.69	55.96	0.441	6.032

It is well known that the brittleness or ductile of materials is very important for its practical application. According to Pugh standards of mechanical behavior of crystals, the ratio of bulk modulus *B* to shear modulus *G* can be used to predict whether a solid material is brittle or ductile, when the ratio *B*/*G* is more than 1.75, it is ductile material, and when the ratio is less than 1.75, it is brittle material[17]. The *B*/*G* values at different pressures are much larger than 1.75. Therefore, it can be concluded that α-Cu_2S crystal is a ductile material.

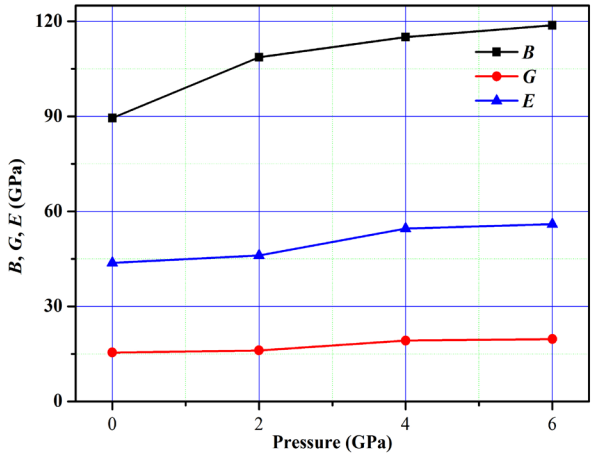

Fig. 7. Effect of pressure on B, G, and E of α-Cu_2S as a function of pressure.

3.4. Optical properties

Fig. 8 shows the relation between the real and imaginary parts of the dielectric function of α-Cu_2S with respect to the photon energy, where the Re curve represents the change of the real part with respect to the photon energy and the Im curve represents the change of the imaginary part with respect to the photon energy. From the graph, we can know that the static permittivity of α-Cu_2S is 24.21, and the real part gets the maximum value at the photon energy of 0.69 eV, then the real part decreases gradually in a fluctuating manner, and the real part gets the minimum value when the photon energy is 9.32 eV, then the real part tends to zero as the photon energy increases, and the photon energy at zero is about 24 eV. The absorption edge of the imaginary part of the dielectric function of α-Cu_2S is obtained at the photon energy of 1.46 eV, which corresponds to the direct optical transition between the bottom of the conduction band and the top of the valence band, the imaginary part has five peaks, which are labeled E_0, E_1, E_2, E_3, E_4, corresponding to the photon energies: 1.46 eV, 4.92 eV, 6.09 eV, 8.52 eV, 10.96 eV, which represent five different interband transitions, respectively.

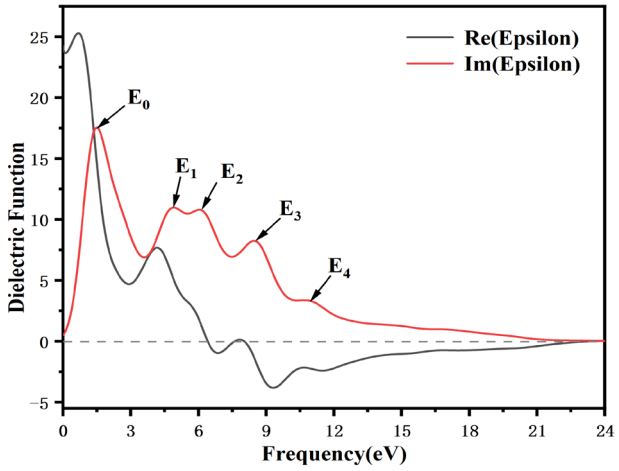

Fig. 8. The real part $\varepsilon_1(\omega)$ and imaginary part $\varepsilon_2(\omega)$ of the dielectric function of α-Cu_2S.

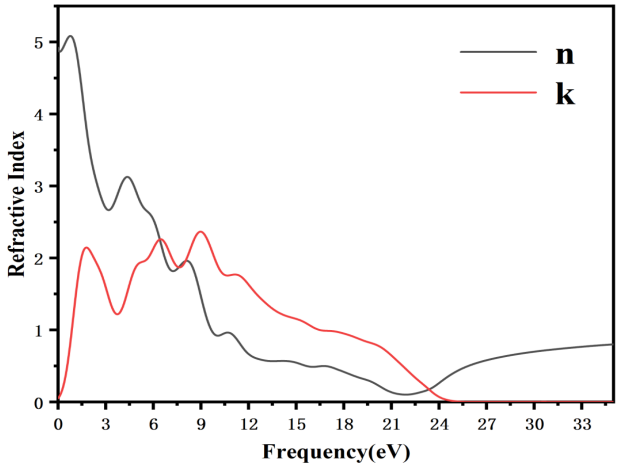

Fig. 9. The refractive index n(ω) and the extinction coefficient k(ω) of the α-Cu_2S.

The complex refractive index is composed of the real part $n(\omega)$ and the imaginary part $k(\omega)$, which is used to describe the propagation velocity of light waves in an absorbing medium, i. e. the refractive index of an absorbing medium. The imaginary part $k(\omega)$ is the extinction coefficient, which is used to describe the energy loss when the photon propagates in the medium. Fig. 9 shows the change of photon energy in the real and imaginary parts of the complex refractive index of α-Cu_2S. From Fig. 9, we can see that the refractive index of α-Cu_2S is $n_0 = 4.86$, the maximum value of n is obtained at the photon energy of 0.78 eV, and then the value of n decreases with the increase of photon energy, at the photon energy of 21.91 eV, the minimum value is obtained, and finally it increases monotonously to 1. The peak value of extinction coefficient k of α-Cu_2S mainly appears in the photon energy range of 1.75 eV ~ 11.25 eV, and the value of k is equal to zero when the photon energy is 25.02 eV.

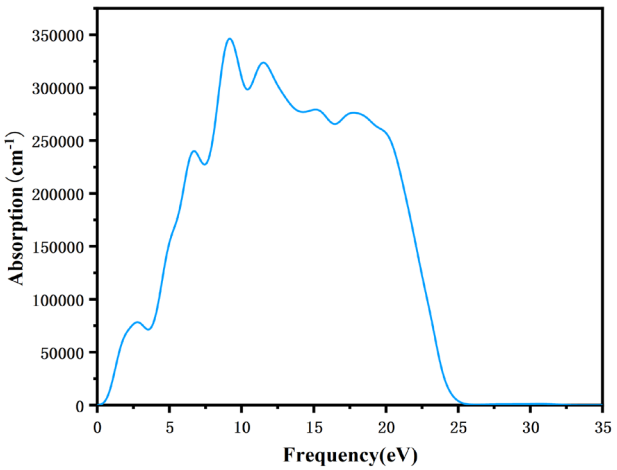

Fig. 10. The absorption coefficient of the α-Cu_2S.

Fig. 10 shows the absorption coefficient of α-Cu_2S as a function of photon energy. It can be seen from Fig. 10 that the absorption coefficient is not zero in the range of photon energy from 0.37 eV to 25.63 eV, the maximum value of 3.46×10^5 cm^{-1} is obtained at the photon energy of 9.16 eV, then the absorption coefficient decreases gradually with the increase of photon energy, and finally the value of 0 cm^{-1} is obtained at the energy of 25.63 eV.

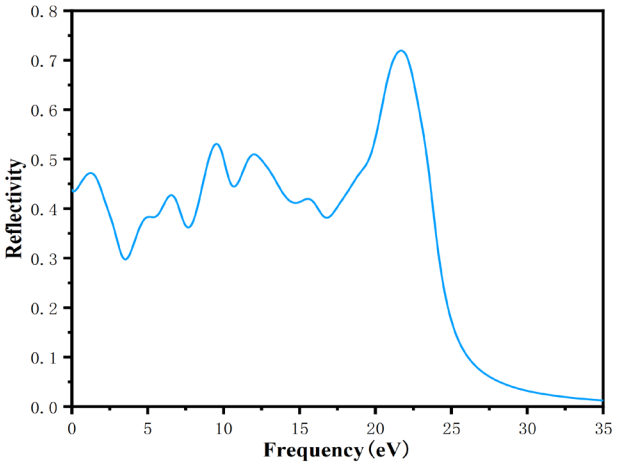

Fig. 11. The reflectivity spectrum R(ω) of the α-Cu_2S.

Fig. 11 shows the reflectivity of α-Cu_2S as a function of photon energy. From this figure, it can be concluded that the static reflectivity $R(0)$ of Cu_2S is 0.438, and the reflectivity curve fluctuates basically up or down 0.4 in the range of photon energy from 0 to 20 eV, only when the photon energy is 21.70 eV, the maximum value of reflectivity is 0.719, and then with the photon energy increasing, the refractive index decreases monotonically to zero.

4. Conclusions

In summary, the electronic structure, mechanical properties and optical properties of α-Cu_2S is studied by density functional theory. The obtained lattice constant of the studied crystal shows that the values are very close to the experimental value. The band and the density of states of the studied crystal is calculated. A series of elastic modulus such as bulk modulus, Young's modulus, shear modulus and poisson's ratio are calculated to study the elastic properties of α-Cu_2S under different pressures. The optical properties of α-Cu_2S crystal, such as dielectric function, refractive index, absorption coefficient and reflectivity were calculated and analyzed.

Acknowledgments

This work was supported by the Huaihua University Double First Class initiative Applied Characteristic Discipline of Control Science and Engineering, Key Laboratory of Intelligent Control Technology for Wuling-Mountain Ecological Agriculture in Hunan Province, and Huai hua Key Laboratory of Agricultural Ecology Prevention and control.

References

[1] S. R. Zhang, D. P. Zeng , L. H. Xie, X. P. Deng, K. H. Song, Chalcogenide Lett. 11, 661(2014)2014

[2]Y. Rodríguez-Lazcano, M. T. S. Nair, P. K. Nair, Mod. Phys. Lett. B, 15, 667(2001); https://doi.org/10.1142/S0217984901002257

[3]W. Septina, S. Ikeda Y. Iga, T. Harada, M. Matsumura,Thin solid films, 550, 700(2014); https://doi.org/10.1016/j.tsf.2013.11.046

[4]J. T-Thienprasert, S. Limpijumnong, Appl. Phys. Lett. , 107, 221905(2015); https://doi.org/10.1063/1.4936760

[5] C. Yan, Z. Su, E. Gu, T. Cao, J. Yang, J. Liu, F. Liu, Y. Lai, J. Li, Y. Liu, RSC Adv., 2,10481 (2012) ; https://doi.org/10.1039/c2ra21554c

[6] K. Ramasamy, B. Tien, P. S. Archana, A. Gupta, Mater. Lett., 2014, 124, 227(2014); https://doi.org/10.1016/j.matlet.2014.03.046

[7]S. Chen, A. Walsh, J. Yang, X. G. Gong, Physical Review B **83,**125201(2011); https://doi.org/10.1103/PhysRevB.83.125201

[8]S. J. Clark, M. D. Segall, C. J. Pickard, Z. Kristallogr 220,567 (2005); https://doi.org/10.1524/zkri.220.5.567.65075

[9] D. Vanderbilt Phys. Rev. B 41, 7892(1990); https://doi.org/10.1103/PhysRevB.41.7892

[10]FJ. P. Perdew, K Burke, M. Ernzerhof Phys. Rev. Lett. 77,3865 (1996); https://doi.org/10.1103/PhysRevLett.77.3865

[11]D.J. Chakrabarti, D.E. Laughlin,,Bulletin of Alloy Phase Diagrams, 4, 255(1983); https://doi.org/10.1007/BF02868665.

[12] Q. Xu, B. Huang, Y.F. Zhao, Y.F. Yan, R. Noufi, S.H. Wei, Appl. Phys. Lett. 100, 061906 (2012);https://doi.org/10.1063/1.3682503

[13] A. Boudjemline, L. Louail , M. Mazharul, B. Diawara, Comp. Mater. Sci., 50, 2280(2011); https://doi.org/10.1016/j.commatsci.2011.03.006

[14] W. Voigt Lehrbuchder Kristallphysik Teubner Leipzig (1928)

[15] A. Reuss , Z. Angew. Math. Mech. 9, 49 (1929); https://doi.org/10.1002/zamm.19290090104

[16] R. Hill, Proc. Phys. Soc. 65, 349 (1952); https://doi.org/10.1088/0370-1298/65/5/307

[17] S. F. Pugh, Philos. Mag. 45, 823 (1954); https://doi.org/10.1080/14786440808520496